On the Efficient Extraction of Entangled Resources

Si-Yi Chen, Angela Sara Cacciapuoti, *Senior Member, IEEE*, Marcello Caleffi, *Senior Member, IEEE*

***Abstract*—In the Quantum Internet, multipartite entanglement enables a rich and dynamic overlay topology, referred to as artificial topology, upon the physical one, that can be exploited for communication purposes. In fact, the ability to extract n-qubits GHZ states and EPR pairs from the original multipartite entangled state constitutes the resource primitives for end-to-end and on-demand quantum communications. Thus, in this paper, we theoretically determine upper and lower bounds for the number of extractable n-qubits GHZ states and EPR pairs involving nodes remote in the artificial topology, as well as the achievable size n of remote GHZ states. The theoretical analysis is then complemented by the proposal of a novel algorithm, which provides in polynomial-time a heuristic solution to the above problem. This is remarkable, since the theoretical problem is NP-complete. The performance analysis demonstrates the proposed algorithm is able to effectively manipulate the original and arbitrary graph state for extracting entanglement resources across remote nodes.**

***Index Terms*—Multipartite Entanglement, Entanglement-Enabled Connectivity, Network Connectivity, Quantum Networks, Quantum Communications, Quantum Internet**

I. Introduction

ENTANGLEMENT shared between more than two parties, known as multipartite entanglement, represents a powerful resource for quantum networks [2]–[10]. It enables a new form of connectivity, referred to as *entanglement-enabled connectivity* [2], [5], which augments the physical topology with virtual links, activated by the entanglement, and referred to as *artificial links*, between pairs of nodes, remote in the physical topology[1], without any additional physical link deployment. Thus, multipartite entanglement enables a richer, dynamic overlay topology, referred to as *artificial topology*, upon the physical one. And this artificial topology can be properly manipulated to account for the dynamics of the node communication needs [12]–[14].

Most of the literature on multipartite entanglement manipulation usually aims at extracting from the initial multipartite state a certain amount, say k, of shared EPR pairs. These k EPR pairs can be subsequently exploited for the parallel "transmission" of k informational qubits, by adopting the quantum teleportation protocol [15]. It is worthwhile to note that the identities of the nodes involved in the k disjoint pairs are fixed, with no possibility of changing them to time-varying communication needs. Differently, the manipulation of an artificial topology for extracting GHZ states [16]–[19] overcomes the above constraint. Specifically, a GHZ state – key for various quantum communication protocols [20]–[24] – represents, from a communication perspective, an artificial subnet, extracted among a certain number of nodes, starting from the original multipartite state. And the rationale for defining a GHZ as subnet rather than link is that it enables the dynamic extraction of an EPR pair between any pair of nodes sharing the original GHZ state. Remarkably, this extraction can happen at run-time, depending on the actual node communication needs. From the above it follows that nodes belonging to an artificial subnet exhibit an *entanglement proximity*, i.e. a distance in terms of entanglement hops, equal to one.

In this context, it is key to observe that having a fully-connected artificial topology among all the network nodes is not reasonable, due the challenges related to (and the complex equipment necessary for) the generation and the control of a high-order multipartite state. Hence, it is more practical and reasonable to assume the presence of nodes that are remote even in the artificial topology. In the remaining part of this work, we focus on this type of nodes, since remote nodes in the artificial topology face reduced communication opportunities compared to nodes already interconnected. As a consequence, artificially interconnecting this type of nodes, not only assures network fairness, but also constitutes a communication primitive for end-to-end and on-demand communications [25]–[29].

Additionally, it is key to observe that the entanglement extraction capabilities of a certain multipartite state heavily depend on the features of this selected state [30]. The original state also affects whether the extractions happen deterministic or probabilistic [5]. Thus, the choice of the initial multipartite state is a key network design choice. A notable class of multipartite entangled states is the *two-colorable graph state* class [31], modeling important communication network topologies, such as grid, star, bistar, linear, even loop, butterfly, cluster networks [12], [13], [29], [32]–[37].

With the above in mind, in this paper we assess the extraction capability of a generic graph state, in terms of "volume", "mass" and "location"[2] of GHZ states and EPR pairs, shared among nodes *remote in the original artificial topology*. And we refer to the aforementioned remote extraction capability for GHZ and EPR states as *remote Gability* and *remote Pairability*, respectively. In a nutshell, we:

- *quantify the volume* of ultimate links via lower bounds, by assessing the extraction EPR capabilities starting from an arbitrary two-colorable graph state;

A preliminary conference version of this work is [1].

The authors are with the www.QuantumInternet.it Group, University of Naples Federico II, Naples, 80125 Italy.

This work has been funded by the European Union under the ERC grant QNattyNet, n.101169850. The work has been also partially supported by PNRR MUR RESTART-PE00000001.

[1]It is worth noting that, in agreement with current quantum technology Technology Readiness Level (TRL), the physical network topology is generally sparse. Thus, it heavily limits the node communication capabilities [11].

[2]We collected and summarized the terms widely exploited in the remaining part of the manuscript in Tab. I.

TABLE I: Adopted terms in entanglement-enabled connectivity domain

Terms	Interpretations
Artificial topology	A virtual network topology, built upon the physical topology, and associated with a certain multipartite entanglement state.
Artificial link	A virtual link, pictorially visualized as an edge between two nodes connected in an artificial topology, corresponds to a CZ interaction between the qubits and denotes the "possibility" of extracting an EPR pair between the two considered nodes. Thus, artificial link and EPR are not synonymous.
Artificial subnet	A virtual subnet, pictorially visualized as a fully connected subgraph in an artificial topology, corresponds to the "possibility" of extracting a GHZ state among the involved nodes.
(Artificial) remote nodes	Non-adjacent nodes in the artificial topology that are not directly connected by an artificial link (Def. 1).
(Artificial) remote subnet	An artificial subnet formed by an independent set of nodes in an artificial topology.
Ultimate artificial links	The actual EPR pairs extracted from the original multipartite state.
Ultimate artificial subnets	The actual GHZ states extracted from the original multipartite state.
Location	The location of an (ultimate) artificial link/subnet refers to the identities of the interconnected nodes.
Volume	The volume of (ultimate) artificial link/subnet refers to the number of EPR pairs / GHZ states that can be *simultaneously* extracted from a given multipartite state. This volume heavily depends on the type and structure of the considered multipartite state, and some of the artificial links are depleted during the extraction process.
Mass	The mass of an (ultimate) artificial subnet refers to the number of interconnected nodes.

- *quantify both volume and mass of ultimate subnets* via lower bounds, by assessing the n-qubit GHZ extraction capabilities for any size n;
- *quantify* the remote Pairability and n-Gability volumes also via theoretical upper bounds.

The theoretical analysis is then complemented by the proposal of a novel algorithm, which provides in polynomial-time a heuristic solution to the above problem. This is remarkable, since the theoretical problem is NP-complete, as better highlighted in the following subsection.

The rest of this manuscript is organized as follows. In Sec. II we first provide the reader with a formal definition of the research problem, along with an overview of the main results derived in the manuscript. In Sec. III, we first present some preliminaries, and then we derive constructive conditions for both the remote Gability and remote Pairability. In Sec. IV, we present the proposed polynomial-time algorithm along with its complexity analysis. In Sec. V, we evaluate the tightness of the constructive derived bounds with respect to general and bipartite graph states.

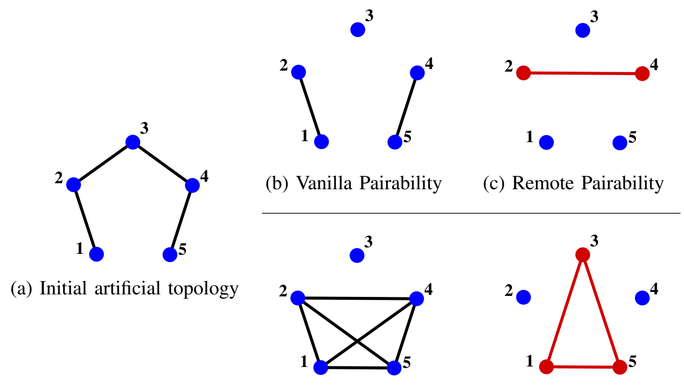

(a) Initial artificial topology

(b) Vanilla Pairability

(c) Remote Pairability

(d) Vanilla Gability

(e) Remote Gability

Fig. 1: *Remote* vs *Vanilla* Pairability and Gability for a 5-qubit linear graph state. (a) The initial artificial topology is a 5-qubit linear graph state. (b) Vanilla Pairability allows extraction of up to two EPR pairs from (a). (c) Remote Pairability enables extraction of only one EPR pair between remote nodes from (a). (d) Vanilla Gability permits extraction of a maximal 4-qubit GHZ state from (a). (e) Remote Gability supports extraction of a maximal 3-qubit GHZ state among remote nodes, corresponding to the maximum independent set in (a).

A. Related Work And Contribution

In [38], it has been shown that the computational complexity of extracting Bell pairs from graph states is NP-complete. And in the same paper, the authors refer to this problem as Bell-VM [38]. Research in this area [33]–[35], [38], [39] has potential applications in point-to-point quantum communication protocols, where the extracted k Bell pairs can be used for the parallel transmission of k informational qubits via teleporting protocol. In particular, in [35], it is showed that N-qubit CSS state can extract k pairs of EPR between k disjoint parties, with k proportional to $\log N$. Extending this idea, [39] determines two families of k-vertex-minor universal graphs based on two-colorable graph states, starting from a $N = O(k^4)$-qubit resource state. Similarly, [33] proposes the Zipper-protocol, enabling the extraction of multiple EPR pairs from a 2D cluster state along the diagonal direction. In contrast, the X-protocol in [34] extracts EPR pairs at predetermined locations while somehow preserving part of the entanglement among remaining qubits.

A related line of research focuses on determining whether a GHZ state can be extracted from a given graph state, by using only local Clifford (LC) operations, local Pauli measurements (LPM), and classical communication (CC). This problem has also been proven to be NP-complete [40]. For ease of reference, we refer to the aforementioned problem as *GHZ-VM problem*. Although the GHZ-VM problem [16]–[19] concerns the extraction of a single GHZ state, it offers a significant advantage over the Bell-VM formulation, since it inherently supports adaptability to the traffic requests. In fact, as mentioned above, a GHZ state allows the dynamic extraction of an EPR pair between any pair of nodes sharing the original GHZ state. And, notably, this extraction can occur at runtime, driven by the actual and potentially time-varying communication needs of the nodes.

It should be emphasized that the existing Bell-VM and GHZ-VM studies lie within the so-called vanilla extractions, as represented in Fig. 1. Specifically, there exists a subtle but key difference between remote and vanilla Gability/Pairability. In fact, in the latter, the extraction is performed regardless of the nodes proximity within the artificial topology. This in turn simplifies the problem with respect to constrain the extraction among nodes that are remote in the artificial topology.

Accordingly, in this paper, we extend the Bell-VM and GHZ-VM approaches to a deeper problem, referred to as *Remote-VM problem*, by determining the number of n-qubit GHZ states and Bell pairs, as well as the mass of GHZ that can be currently extracted among remote nodes of a given graph state, by using only single-qubit Clifford operations, single-qubit Pauli measurements, and classical communication.

The difference between Remote-VM, existing Bell-VM and GHZ-VM is pictorially represented in Fig. 2. Specifically, while both Bell-VM and GHZ-VM are *existential* decision problems (determining whether a resource state can be extracted), the Remote-VM problem belong to the *counting problem class*. Thus, it not only resolve the existence, but also determine the exact extractable resources. It is important to note that Bell-VM and GHZ-VM have been proved to be NP-complete [38], [40]. Given that our problem introduces an additional constraint on top of Bell-VM and GHZ-VM, the Remote-VM problem is evidently at least in the NP-complete complexity class.

More into details, the concurrent extraction of remote GHZ states and Bell pairs is equivalent to identifying disjoint independent sets in the original artificial topology. Leveraging this equivalence, the Remote-VM problem is reminiscent of the well-studied problem in the classical domain referred as #IS problem [41], which is #P-complete even when restricted to bipartite graphs [42], [43]. However, solving a counting problem in the quantum domain is not only linked to the structure of the graph, as in the classical #IS problem. Indeed the Remote-VM problem is constrained also by the operational limitations inherent to quantum systems. This additional constraint significantly increases the complexity of the problem, although it is out of the scope of this paper to study its complexity class.

With the above in mind, in the paper, in addition to the theoretical contribution highlighted in the Introduction, we also propose an heuristic solution for the NP-complete *Remote-VM problem*. Specifically:

- We propose a polynomial-time algorithm for the Remote-VM (see Sec. IV-A), by exploiting graph-theory tools and only LC + LPM + CC.
- The algorithm facilitates the extraction of both n-qubit GHZ states and EPR pairs among remote nodes, by extending the extraction capabilities beyond a set of apriori selected EPR pairs or a specific GHZ state.
- The algorithm is able to provide the three aforementioned parameters, namely volume, locations, and maximum mass, that rule the remote extraction.

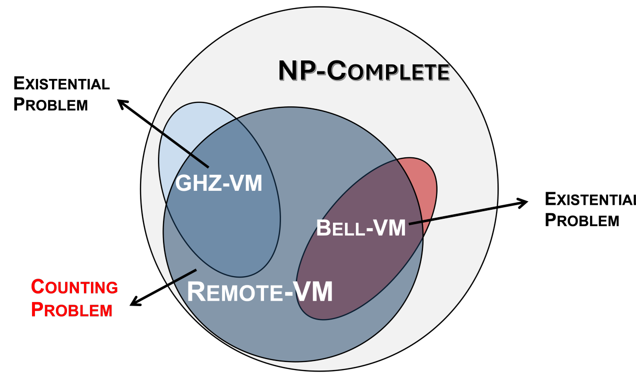

Fig. 2: Venn diagram for the relationship between GHZ-VM, BELL-VM and REMOTE-VM (our research problem).

- We evaluate the extractable volume for both remote Gability and remote Pairability, as well as the maximum mass for remote Gability, in general graph states. The analysis is conducted on representative Internet inspired artificial topologies and the results demonstrate their effectiveness (see Sec. V).

To the best of our knowledge, this is the first paper rigorously investigating the extraction of remote entangled resources, while also providing an efficient polynomial-time procedure for its realization.

II. Research Problem

We consider the worst case scenario, where each qubit of the graph state is distributed to each network node. And we equivalently refer to node i or to vertex v_i associated with the qubit of the graph state $|G\rangle$ stored at such a node. To formally define our research problem, the following definitions are preliminary.

Definition 1 (**Remote Nodes**). Given a N-qubit graph state $|G\rangle$ and its corresponding graph $G = (V, E)$, two network nodes i and j are defined as *remote* if the corresponding vertices v_i, v_j are non-adjacent in G, i.e., if[3]:

$$(v_i, v_j) \notin E. \tag{1}$$

Throughout this paper, the notions of "*remoteness*" and its counterpart, *adjacency*, do not refer to the physical proximity of network nodes. Instead, they describe "*entangled proximity*", that is, proximity within the artificial topology associated with the graph G [2], [12]. Indeed, the presence of an edge within two vertices in G represents an Ising interaction between the corresponding qubits of the graph state [44], [45]. As a direct consequence of a graph state definition, it is evident that the graph associated to the graph state is a connected graph, meaning that a vertex is at least connected with another vertex. Two nodes are considered remote if they are not adjacent in this artificial topology. A subset of remote

[3]In the following, with a small notation abuse, we denote un-directed edges as (v_i, v_j) – rather than with angle brackets as $\{v_i, v_j\}$ – for notation simplicity.

nodes is referred to "*Remote Subnet*", as formally defined in Def. 2.

Definition 2 (**Remote Subnet**)**.** Given a N-qubit graph state $|G\rangle$ and its corresponding graph $G = (V, E)$, a subset of network nodes $\tilde{V} \subset V$ is defined as *remote subnet* if the following condition holds:

$$\forall\, v_i, v_j \in \tilde{V} : (v_i, v_j) \notin E. \tag{2}$$

Stemming from the previous two definitions, we can now define the two main connectivity metrics. These two metrics focus on the quantum communication resources, i.e., GHZs and EPRs, that can be concurrently extracted among remote nodes in the artificial topology.

Definition 3 (**$r_g(n)$: remote n-Gability**)**.** The remote n-Gability of an N-qubit graph state $|G\rangle$ denotes the volume of n-qubit GHZ states, with $n \leq N$, that can be eventually extracted among remote subnets via LC + LPM + CC operation. In the following, we denote the volume of n-qubit GHZ states as $r_g(n)$.

From Def. 3, it results that when it comes to GHZ states, there exist two dimensions that we must account for: the **volume**, similarly to EPRs, and the **mass** of each extracted GHZ, namely, the size of the GHZ in terms of qubit number. These two dimensions map into *the number of the artificial subnets* that can be simultaneously extracted from the initial graph $|G\rangle$, and into *the number of interconnected nodes in each subnet*. The third dimension, namely *location*, is essential for both remote Pairability and n-Gability. Specifically, it plays a critical role in leveraging entangled resources by enabling the unambiguous identification of the participating nodes within the quantum states.

Remark. Since an EPR pair is a special case of a GHZ state with two qubits, the case of $r_g(2)$ is essentially a special instance of remote n-Gability. We refer to this as remote Pairability, which is formally defined in Def. 4.

Definition 4 (**r_e: remote Pairability**)**.** The remote Pairability of an N-qubit graph state $|G\rangle$ denotes the volume of EPR pairs that can be eventually extracted between remote nodes via LC + LPM + CC operation. In the following, we denote the volume of EPRs as r_e, by omitting the dependence on $|G\rangle$ for the sake of notation brevity.

It is worthwhile to mention that solving the Gability problem is more difficult than solving the Pairability problem, and the following inequality holds for the volume whenever $n > 2$:

$$r_g(n) \leq r_g(n-1) \leq r_g(2) \triangleq r_e \tag{3}$$

Stemming from the concept of remote n-Gability and Pairability in Defs. 3 and 4, we can now formally define our research problem.

Research Problem (Remote-VM problem)**.** Given a graph state $|G\rangle$ distributed across the network nodes, we determine the volume, location and maximum mass of n-qubit GHZ states and EPR pairs, extractable among remote nodes, by using only single-qubit Clifford operations, single-qubit Pauli measurements and classical communications.

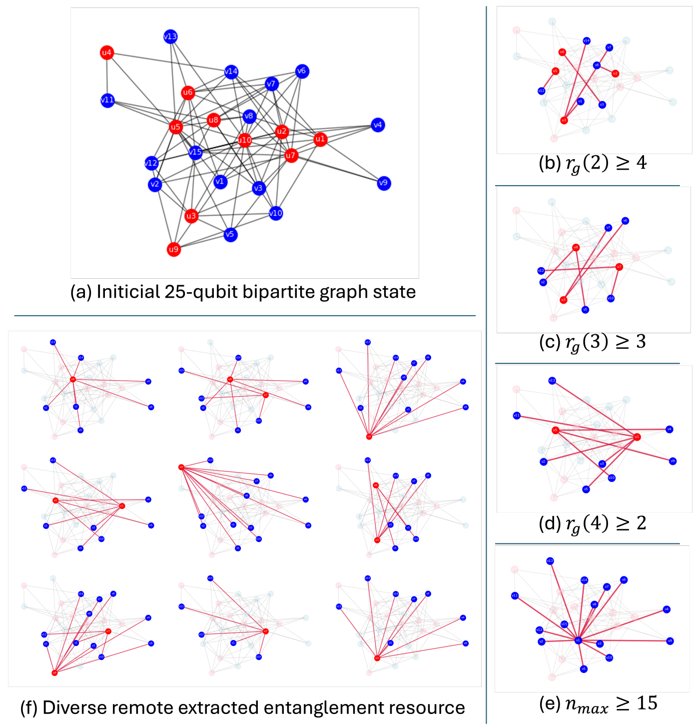

Fig. 3: Pictorial representation of the research problem. (a) The initial 25-qubit bipartite graph state $|G\rangle$. The goal is to constructively address the Remote-VM problem: determining the bound for the volume of extractions can be performed simultaneously from $|G\rangle$, and the bound for the maximum mass of remote GHZ states that can be extracted, and identifying (location) the remote nodes involved in these extractions. (b) A solution to the Remote Pairability problem, identifying pairs of remote nodes that can be entangled. (c–d) Examples for the Remote n-Gability problem, with $n = 3, 4$. (e) Extraction of a 15-qubit remote GHZ state, representing the lower bound of maximum achievable mass of a remote GHZ state from the initial graph. (f) Illustration of diverse extracted remote resources obtained from $|G\rangle$.

As aforementioned, this problem is NP-complete. Thus, we theoretically derive bounds for remote pairing and n-ability for an arbitrary graph state. Specifically, our goal is to determine bounds for:

i) the volume $r_g(n)$ for any value of n, as well as the locations of the remote nodes eventually sharing the GHZ states;
ii) the mass of the remote n-Gability;
iii) and the volume r_e of the remote Pairability, as well as the locations of the remote nodes eventually sharing the EPR pairs.

We underline that the derived lower bounds are far from being only theoretical, since they are derived by individuating the locations of the nodes that share the extracted EPRs/GHZs. Hence, these bounds are *constructive* in the sense that not only they determine whether a solution exists, but they also construct the solution explicitly.

In Fig. 3, we provide a pictorial representation of the formulated research problem to better grasp the implications of the remote extractions from a network perspective.

III. Remote Pairability and Remote n-Gability

Here, we first provide some preliminaries in Sec. III-A. Then, in Sec. III-B we derive the remote extraction conditions for both remote n-Gability and *Pairabilty* for two-colorable graph state $|G\rangle$, in Lemmas 1 and 2, respectively. And we also provide the bound for maximum mass n_{max} for remote G-ability in Lemma 3.

A. Preliminaries

We first introduce several fundamental definitions from graph theory, including the concepts of maximum degree and maximum independent set. These metrics play a crucial role in characterizing entangled proximity in artificial topologies and directly influence the achievable n-Gability and Pairability in the Remote-VM problem.

Definition 5 (**Maximum degree**). The maximum degree of a graph $G = (V, E)$, denoted by $\Delta(G)$, is the largest degree of any vertex in V:

$$\Delta(G) = \max\{\deg(v) \mid v \in V\} \tag{4}$$

with $\deg(v)$ is the number of neighbors of vertex v in G.

Definition 6 (**Maximum Independent set**). A maximum independent set is the independent set of largest size for a given graph G. This size is called the independence number of G, denoted by $\alpha(G)$.

Remark. Remote n-Gability relies on identifying independent sets of size n in the artificial topology, as each of such sets may enable the extraction of a remote n-qubit GHZ state. The larger is the independent set permitted by the artificial topology, the greater is the mass of the extracted remote GHZ state. As a result, the size $\alpha(G)$ of the maximum independent set determines the theoretical upper bound for the mass of a remote GHZ states.

As aforementioned, we focus on two-colorable[4] graph states. This choice is not restrictive, since any graph state can be converted in a two-colorable one under relaxed conditions [30], [46]. Furthermore, two-colorable graphs model a wide range of important communication network topologies, such as butterfly, bistar, tree, linear, even loop, grid, star, cluster networks, highly exploited in entanglement-based communication protocols [12], [13], [29], [32]–[37]. In addition, two-colorable graph states are local-unitary (LU) equivalent to Calderbank-Shor-Steane (CSS) states, which are important in quantum error correction strategies [47]–[49]. Formally, we have the following definition.

[4] In principle, coloring assigns colors to arbitrary elements of a graph according to arbitrary partition constrains. In the following, we adopt the most widely-used partition constraint based on vertex adjacency, since other coloring problems can be easily transformed into a vertex coloring problem.

Definition 7 (**Two-colorable Graph** or **Bipartite Graph**). A graph $G = (V, E)$ is two-colorable if the set of vertices V can be partitioned into two subsets $\{P_1, P_2\}$ so that there exist no edge in E between two vertices belonging to the same subset. Two-colorable graph $G = (V, E)$ can be also denoted as $G = (P_1, P_2, E)$.

Definition 8 (**Star vertex**). Given a two-colorable graph $G = (P_1, P_2, E)$, the vertex v_i belonging to partition P_i is defined as star vertex if its neighborhood $N(v_i)$ coincides with the opposite partition $P_j \stackrel{\triangle}{=} V \setminus P_i$, i.e.,:

$$N(v_i) \stackrel{\triangle}{=} \big\{v_j \in V : (v_i, v_j) \in E\big\} \equiv V \setminus P_i \stackrel{\triangle}{=} P_j. \tag{5}$$

Remark. We underline that our definition of star vertex is not the common one used in graph theory, where a star vertex denotes a vertex connected to all the other vertices in V. In fact, our definition is related to the vertex partitioning, and thus, our star vertex undergoes the coloring constraint. Consequently, the star vertex is not connected to the vertices belonging to its own partition.

In the following, for the sake of notation simplicity, we denoted with $S_1 \subseteq P_1$ and $S_2 \subseteq P_2$ the set of star vertices in the two partitions, i.e.:

$$S_1 = \big\{v_i \in P_1 : N(v_i) = P_2\big\}, \tag{6}$$

$$S_2 = \big\{v_j \in P_2 : N(v_j) = P_1\big\}, \tag{7}$$

and, accordingly, by denoting the remaining vertices, i.e. non-star vertices, in each partition as V_1 and V_2, we can adopt the following labeling for the two-colorable graph $G = (P_1, P_2, E)$:

$$P_1 = S_1 \cup V_1 \tag{8}$$
$$\text{with } S_1 = \{s_1^1, \cdots, s_1^{k_1}\} \wedge V_1 = \{v_1^1, \cdots, v_1^{n_1}\},$$

$$P_2 = S_2 \cup V_2 \tag{9}$$
$$\text{with } S_2 = \{s_2^1, \cdots, s_2^{k_2}\} \wedge V_2 = \{v_2^1, \cdots, v_2^{n_2}\},$$

with $|P_1| = n_1 + k_1$ and $|P_2| = n_2 + k_2$.

Definition 9 (**Opposite Remote-Set**). Given a two-colorable graph $G = (P_1, P_2, E)$, the *opposite remote set* of the arbitrary vertex $v_i \in P_i$, with $i \in \{1, 2\}$, is the set $\overline{N}(v_i)$ of remote vertices of v_i belonging to the other partition:

$$\overline{N}(v_i) \stackrel{\triangle}{=} \big\{v_j \in P_j \neq P_i : (v_i, v_j) \notin E\big\}. \tag{10}$$

The term "opposite" in Def. 9 is used to highlight that the remote nodes belong to different partitions. This will be exploited in the next sections for carrying the theoretical analysis. Clearly, vertices belonging to the same partition are remote *per se*, as a consequence of the two-colorable graph state definition. The concept of the opposite remote set can be extended from individual vertices to subsets of vertices within the same partition. For any subset $A \subseteq P_i$, the union and

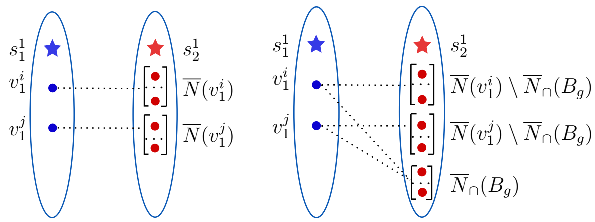

(a) (b)

Fig. 4: Pictorial representation for the conditions of Lemmas 1 and 2. Dashed lines denote opposite remote sets (Def.9), where a dashed line from a vertex to a set of vertices in squared parentheses indicates remote subnets. (a) In G, vertices v_1^i and v_1^j in V_1 satisfy (15), so $A_g = \{v_1^i, v_1^j\}$ by Lem.1. (b) In G, v_1^i and v_1^j in V_1 satisfy (20), so $B_g = \{v_1^i, v_1^j\}$ by Lem. 2.

intersection opposite remote sets are defined respectively as:

$$\overline{N}_\cup(A) \triangleq \bigcup_{v_i \in A} \overline{N}(v_i) \tag{11}$$

$$\overline{N}_\cap(A) \triangleq \bigcap_{v_i \in A} \overline{N}(v_i) \tag{12}$$

B. Remote Extraction Conditions

We provide two sufficient conditions in Lem. 1 and Lem. 2 for remote n-Gability in two-colorable graph states $|G\rangle$, where remote Pairability is treated as the special case of n-Gability for $n = 2$. And, a pictorial representation of the aforementioned conditions is given in Fig. 4.

Lemma 1 (**Remote n-Gability: Condition I**). *Let $|G\rangle$ be a two-colorable graph state, with corresponding graph $G = (P_1, P_2, E)$. A sufficient condition for concurrently extracting $\dot{r}_g(n)$ GHZ states, each involving n qubits, is that $\dot{r}_g(n)$ vertices in one partition have pairwise disjoint opposite remote sets of cardinality at least $n-1$, and that there exists at least one star vertex in each partition. Formally:*

$$\begin{aligned} &\exists S_1, S_2 \neq \emptyset, \exists A_g \subseteq V_i, \text{with } |A_g| = \dot{r}_g(n): \\ &|\overline{N}(v_i)| \geq n-1, \forall v_i \in A_g \ \wedge \\ &\overline{N}(v_i) \cap \overline{N}(v_j) \equiv \emptyset, \forall v_i, v_j \in A_g, v_i \neq v_j. \end{aligned} \tag{13}$$

Proof: Please refer to App. A. ■

Since an EPR pair can be regarded as a degenerate case of a GHZ state involving two qubits, the sufficient condition in Lemma 1 with $n = 2$ applies directly to the concurrent extraction of $\dot{r}_g(2)$ EPR pairs. This result is formally stated in Corollary 1.

Corollary 1 (**Remote Pairability: Condition I**). *Let $|G\rangle$ be a two-colorable graph state, with corresponding graph $G = (P_1, P_2, E)$, and let A_g denote the set defined in (13), for $n = 2$. A sufficient condition for concurrently extracting $\dot{r}_g(2)$ EPR pairs among remote nodes is that $\dot{r}_g(2)$ vertices in A_g have disjoint opposite sets of cardinality at least 1, and that there exists at least one star vertex in each partition.*

Proof: The proof follows by reasoning as in App. A for $n = 2$. ■

Lemma 2 (**Remote n-Gability: Condition II**). *Let $|G\rangle$ be a two-colorable graph state, with corresponding graph $G = (P_1, P_2, E)$. A sufficient condition for concurrently extracting $\ddot{r}_g(n)$ n-GHZ states is that $\ddot{r}_g(n)$ vertices in one partition have opposite remote sets that share only one unique intersection, with each opposite remote set retaining at least $(n-1)$ vertices after excluding the common intersection, and that there exists at least one star vertex in each partition. Formally:*

$$\exists S_1, S_2 \neq \emptyset, \exists! \overline{N}_\cap(B_g), \text{ with } B_g \subseteq V_i \text{ and } |B_g| = \ddot{r}_g(n): \tag{14}$$

$$\begin{aligned} &|\overline{N}(v_i) \setminus \overline{N}_\cap(B_g)| \geq n-1, \forall v_i \in B_g \ \wedge \\ &\left(\overline{N}(v_i) \setminus \overline{N}_\cap(B_g)\right) \cap \left(\overline{N}(v_j) \setminus \overline{N}_\cap(B_g)\right) \equiv \emptyset, \forall v_i, v_j \in B_g, v_i \neq v_j. \end{aligned}$$

with $\overline{N}_\cap(B_g) \subset P_j \neq P_i$ defined in (12).

Proof: By removing $\overline{N}_\cap(B_g)$, the vertices in B_g will satisfy Lem. 1, becoming as A_g. Please refer to App. A. ■

Similarly, the sufficient condition in Lemma 2 with $n = 2$ applies directly to the concurrent extraction of $\ddot{r}_g(2)$ EPR pairs. This result is formally stated in Corollary 2.

Corollary 2 (**Remote Pairability: Condition II**). *Let $|G\rangle$ be a two-colorable graph state, with corresponding graph $G = (P_1, P_2, E)$ and let B_g denote the set defined in* (14) *for $n = 2$. A sufficient condition for concurrently extracting $\ddot{r}_g(2)$ EPR pairs, is that there exist $\ddot{r}_g(2)$ vertices in B_g and that there exists at least one star vertex in each partition.*

For an arbitrary graph state, it may happen that only one partition or no partition in $|G\rangle$ contains star vertices. Thus, neither Lemmas 1 nor 2 can be exploited to assess n-Gability and pairability. Here, we work toward such an issue by introducing additional graph manipulations, as formally defined in Cor. 3.

Corollary 3. *Let $|G\rangle$ be a two-colorable graph state, with corresponding graph $G = (P_1, P_2, E)$, where $P_j = V_j$, namely P_j contains no star vertices. G can be reduced to a graph G' – vertex minor of G – characterized by a star vertex in partition P_j, as follows:*

$$G' = G \setminus \overline{N}(v_j^i) \tag{15}$$

with $v_j^i \in P_j$ denoting the new star vertex.

Proof: By removing the opposite remote-set of v_j^i, the neighborhood $N(v_j^i)$ in the resulting graph G' coincides with $V_{\bar{j}}$. Hence v_j^i becomes a star vertex in P_j according to Def. 8. ■

By exploiting Cor. 3, each partition of a general graph state can be forced to contain at least one star vertex. This structural property serves as a necessary condition for both Lemma 1 and Lemma 2. With this in mind, let us denote with $\mathcal{A}_g$ the collections of sets satisfying (13), while $\tilde{\mathcal{A}}_g \subseteq \mathcal{A}_g$ comprises the maximal-cardinality subsets of size $\tilde{\dot{r}}_g(n)$, i.e.:

$$\tilde{\mathcal{A}}_g = \{\tilde{A}_g \in \mathcal{A}_g : |\tilde{A}_g| = \tilde{\dot{r}}_g(n)\}, \text{with } \tilde{\dot{r}}_g(n) \triangleq \max_{A_g \in \mathcal{A}_g} \{|A_g|\}. \tag{16}$$

Similarly $\mathcal{B}_g$ denotes the collections of sets satisfying (14), while $\tilde{\mathcal{B}}_g \subseteq \mathcal{B}_g$ comprises the maximal-cardinality subsets of size $\tilde{\tilde{r}}_g(n)$, i.e.:

$$\tilde{\mathcal{B}}_g = \{\tilde{B}_g \in \mathcal{B}_g : |\tilde{B}_g| = \tilde{\tilde{r}}_g(n)\}, \text{with}\, \tilde{\tilde{r}}_g(n) \triangleq \max_{B_g \in \mathcal{B}_g} \{|B_g|\}. \tag{17}$$

By accounting for (16) and (17), it results that the volume of remote n-Gability and remote Pairability for a general two-colorable graph state are theoretically lower- and upper-bounded as follows, respectively:

$$r_g^{\ell_T}(n) \triangleq \max\{\tilde{r}_g(n), \tilde{\tilde{r}}_g(n)\} \leq r_g(n) \leq \lfloor \frac{N}{n} \rfloor, \tag{18}$$

$$r_e^{\ell_T} \triangleq \max\{\tilde{r}_g(2), \tilde{\tilde{r}}_g(2)\} \leq r_g(2) \leq \lfloor \frac{N}{2} \rfloor. \tag{19}$$

Lemma 3 (**Mass $n_{\mathbf{max}}$**). *Given a N-qubit two-colorable graph state $|G\rangle$, with corresponding graph $G = (P_1, P_2, E)$, the highest mass n_{max} of an extractable GHZ state among remote nodes satisfies the following inequality:*

$$n^{\ell}_{max} \triangleq \Delta(G) \leq n_{max} \leq \alpha(G) < N. \tag{20}$$

with $\Delta(G)$, $\alpha(G)$ given in Def. 5 and Def. 6, respectively.

Proof: Let us denote with $v_i \in G$, a vertex characterized by $\deg(v_i) = \Delta(G)$. Performing Pauli-y measurement on v_i yields to the extraction of a GHZ state among all the neighbors of v_i. Hence n_{max} is at least $\Delta(G)$. We define the constructive lower bound of n_{max} to be $\Delta(G)$. The theoretical upper bound, $\alpha(G)$ directly follows from the remark after Def. 6. ■

IV. ALGORITHM

In the previous section, we established theoretical bounds for the volume of remote n-Gability and remote pairabilty, arising directly from the sufficient conditions established in Lemmas 1 and 2. However, given the computational complexity of determining $\tilde{r}_g(n), \tilde{\tilde{r}}_g(n)$, here we provide constructive lower bounds for both remote n-Gability and remote Pairability, by designing an efficient algorithm for the extraction of remote entanglement resources. Then, in Sec. IV-B, we prove that such an algorithm exhibits a polynomial-time complexity.

A. Algorithm Design

The proposed algorithm for remote entanglement extraction is described in Algorithm 1, organized into three steps:

- *Step 1: Approximating the maximum mass n_{max} of a remote GHZ with its lower bound in* (20).
  Let G be the corresponding graph of $|G\rangle$. If G does not have at least one star vertex in a certain partition P, then one vertex is updated as new star vertex in partition P (Line 1-6). Then, by searching for the vertex with maximum degree in the star set $(S_1 \cup S_2)$, we approximate the maximum mass n_{max} with its lower bound $n^{\ell}_{max} \triangleq \Delta(G)$, as proved in Lemma 3.
- *Step 2: Computing the volume $r^{\ell}_g(n)$ of extractable remote GHZ states, each of mass n.*
  This step is decomposed in two sequential sub-steps: *Step 2.1* deriving an initial estimation $\tilde{r}_g(n)$ of the volume; *Step 2.2* iteratively refining $\tilde{r}_g(n)$ to obtain a more precise volume estimation $r^{\ell}_g(n)$, as detailed in the following.
  - *Step 2.1*: Two sets A_g and B_g are randomly chosen in G, by satisfying equations (13) and (14), respectively. By comparing the cardinality of these two set,

Algorithm 1 **`Remote Extraction`**(G, n)

Input: two-colorable graph $G = (P_1, P_2, E)$
Output: $n^{\ell}_{max}, r^{\ell}_g(n), \mathcal{L}$

▷ ***Step 1: Approximating the maximum mass*** n_{max} ***with the lower bound in*** (20)
1: **for** P in (P_1, P_2) **do**:
2: **if** $\nexists v_i \in P$ with $N(v_i) = \bar{P}$ **then** ▷ *Partition P lacks star vertex*
3: $v_i \leftarrow \arg\max_{v \in P} \deg(v)$
4: $S, G \leftarrow S \cup \{v_i\}, G \setminus \overline{N}(v_i)$
5: **end if** ▷ *Updated v_i into star set S in partition P*
6: **end for** ▷ *$S_{1(2)}$, $P_{1(2)}$, $V_{1(2)}$ given in* (6)-(9)
7: $n^{\ell}_{max} \leftarrow \max\{\deg(v) \mid v \in (S_1 \cup S_2)\}$

▷ ***Step 2: Computing the volume*** $r^{\ell}_g(n)$

▷ *Step 2.1: Drive initial $\tilde{r}_g(n) = |\tilde{A}_g| = \max\{|A_g|, |B_g|\}$ by random choosing A_g, B_g in one partition*
8: $A_g \leftarrow$ random.choice ($A_g \subseteq V_1 : A_g$ satisfy (13) in G)
9: $B_g \leftarrow$ random.choice ($B_g \subseteq V_1 : B_g$ satisfy (14) in G)
10: **if** $|B_g| > |A_g|$ **then**
11: $G, \tilde{A}_g \leftarrow G \setminus \overline{N}_{\cap}(B_g), B_g$
12: **else**
13: $G, \tilde{A}_g \leftarrow G, A_g$
14: **end if**

▷ *Step 2.2: Obtain $r^{\ell}_g(n) = |\hat{A}_g|$ after updating $\tilde{A}_g$ to $\hat{A}_g$*
15: $\mathtt{A}, \bar{\mathtt{A}}2\mathtt{A} \leftarrow$ EXPANDA$(G, n, \tilde{A}_g)$
16: **while** $\mathtt{A} \neq \emptyset$ **do**
17: **if** $\exists v_i \in \mathtt{A}$ with $|\mathtt{A}(v_i)| = 0$ **then**
18: $\tilde{A}_g \leftarrow \tilde{A}_g \cup \{v_i\}$ ▷ *Add v_i to $\tilde{A}_g$*
19: **else**
20: Select any $v_i \in \mathtt{A}$
21: **if** $|\bar{\mathtt{A}}2\mathtt{A}(v_i)| = 0$ **then**
22: $G \leftarrow G \setminus \big(\overline{N}(v_i) \cap \overline{N}_{\cup}(\mathtt{A}(v_i))\big)$
23: $\tilde{A}_g \leftarrow \tilde{A}_g \cup \{v_i\}$ ▷ *Add v_i to $\tilde{A}_g$*
24: **else if** $|\bar{\mathtt{A}}2\mathtt{A}(v_i)| = 1$ **then**
25: $v_j \leftarrow \arg_{v_i} |\bar{\mathtt{A}}2\mathtt{A}(v_i)| = 1$
26: $G \leftarrow G \setminus \big(\overline{N}(v_i) \cap \overline{N}_{\cup}(\mathtt{A}(v_i))\big) \setminus \{v_j\}$
27: $\tilde{A}_g \leftarrow (\tilde{A}_g \cup \{v_i\}) \setminus \{v_j\}$ ▷ *Replace v_j with v_i in $\tilde{A}_g$*
28: **end if**
29: **end if**
30: $\mathtt{A}, \bar{\mathtt{A}}2\mathtt{A} \leftarrow$ EXPANDA$(G, n, \tilde{A}_g)$
31: **end while**
32: $\hat{A}_g, r^{\ell}_g(n) \leftarrow \tilde{A}_g, |\tilde{A}_g|$

▷ ***Step 3: Identifying the location*** $\mathcal{L}$
33: $\mathcal{L} \leftarrow \Big\{ v_i \mapsto \overline{N}(v_i) \;\Big|\; v_i \in \hat{A}_g \Big\}$
34: **return** $n^{\ell}_{max}, r^{\ell}_g(n), \mathcal{L}$

Function 1 $\texttt{ExpandA}(G, n, \tilde{A}_g)$

$\bar{A} \leftarrow \{v_i \in V_i \setminus \tilde{A}_g : (|\overline{N}(v_i)| \geq (n-1)) \wedge (\overline{N}(v_i) \not\subseteq \overline{N}_{\cup}(\tilde{A}_g))\}$
$\texttt{A}, \texttt{B2A}, \bar{\texttt{A}}\texttt{2A} \leftarrow \emptyset, \emptyset, \emptyset$
for $v_i \in \bar{A}$ **do**
  $\texttt{B2A}(v_i) \leftarrow \{v_j \in \tilde{A}_g : \overline{N}(v_j) \cap \overline{N}(v_i) \neq \emptyset\}$
  $\bar{\texttt{A}}\texttt{2A}(v_i) \leftarrow \{v_j \in \tilde{A}_g : \overline{N}(v_j) \subseteq \overline{N}(v_i)\}$
end for
▷ *Find* $\texttt{A}(v_i)$ *from* $\texttt{B2A}(v_i)$*, which can be combined with* v_i *to form* B_g*, satisfying Lem. 2.*
for $v_i \in \texttt{B2A}$ **do**
  if $|\bar{\texttt{A}}\texttt{2A}(v_i)| \leq 1$ **and** $\forall v_k \in \texttt{B2A}(v_i) \setminus \bar{\texttt{A}}\texttt{2A}(v_i), \{v_i, v_k\}$ satisfies (14) in G **then**
    $\texttt{A}(v_i) \leftarrow \texttt{B2A}(v_i) \setminus \bar{\texttt{A}}\texttt{2A}(v_i)$
  end if
end for
return $\texttt{A}, \bar{\texttt{A}}\texttt{2A}$

an initial estimation $\tilde{r}_g(n)$ of the volume is provided:

$$\tilde{r}_g(n) = |\tilde{A}_g| \triangleq \max\{|A_g|, |B_g|\}. \quad (21)$$

– *Step 2.2*: It consists of an iterative refinement of $\tilde{A}_g$, through a stepwise expansion in lines 15 - 31, to obtain a more granular value $r^{\ell}_g(n)$ of the extractable volume, as illustrated pictorially in Fig. 5. This is achieved by calling the function "ExpandA", which iteratively (within the WHILE loop, lines 16 - 31) scans all the vertices not in $\tilde{A}_g$ (constituting the $\overline{A}$ set in the function "ExpandA") to build an expanded set $\tilde{A}_g$ (lines 18 and 23) of higher cardinality. In particular, $\tilde{A}_g$ is updated either by directly adding $v_i \in \overline{A}$ to $\tilde{A}_g$ (as depicted in Fig. 5a and 5b), or by replacing "weaker" (in terms of opposite remote-set) vertices in the original $\tilde{A}_g$ with vertices in $\overline{A}$ (as depicted in Fig. 5c). At line 32, the expanded $\tilde{A}_g$ is stored in $\hat{A}_g$. The cardinality, $r^{\ell}_g(n)$, of the output $\hat{A}_g$ is the final volume for the remote n-Gability, i.e., by accounting for (21), it results:

$$r^{\ell}_g(n) = |\hat{A}_g| \geq |\tilde{A}_g| = \tilde{r}_g(n) \text{ in (21)}. \quad (22)$$

Notably, $r^{\ell}_g(n)$ in (22) serves as constructive lower bound for the volume of remote n-Gability.

- *Step 3: Identifying the identities of the nodes involved in the entangled resource.*
The location $\mathcal{L}$ of the extracted entangled resources among remote nodes is determined by mapping each node v_i in the set $\hat{A}_g$ to its opposite remote-set $\overline{N}(v_i)$. In other words, each extracted GHZ state is identified by $\{v_i, \overline{N}(v_i)\}$, with $v_i \in \hat{A}_g$.

Clearly, Alg. 1 also provides a constructive strategy for the remote Pairability, when $n = 2$.

B. Algorithm Complexity Analysis

Here, we analyze the complexity of Algorithm 1. Let us assume, without any loss in generality, that the two-colorable graph $G = (P_1, P_2, E)$ is characterized by having $|P_1| \leq |P_2|$, with P_1 and P_2 defined in (8) and (9).

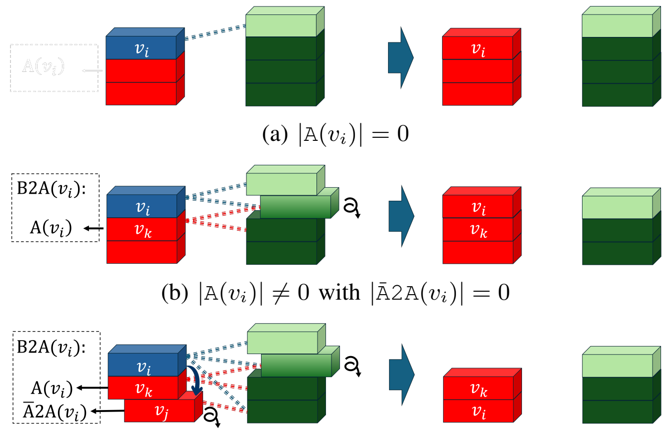

(a) $|\texttt{A}(v_i)| = 0$

(b) $|\texttt{A}(v_i)| \neq 0$ with $|\bar{\texttt{A}}\texttt{2A}(v_i)| = 0$

(c) $|\texttt{A}(v_i)| \neq 0$ with $|\bar{\texttt{A}}\texttt{2A}(v_i)| = 1$

Fig. 5: Pictorial representation of Step 2.2 in Algorithm 1. Dashed lines denote opposite remote sets (Def. 9). **(a)** In the WHILE loop, a vertex v_i with $|\texttt{A}(v_i)| = 0$ (blue brick) is identified and added to $\tilde{A}_g$ (red bricks). **(b)** When no v_i with $|\texttt{A}(v_i)| = 0$ exists, a vertex v_i with $|\bar{\texttt{A}}\texttt{2A}(v_i)| = 0$ is found. After removing $\overline{N}(v_i) \cap \overline{N}_{\cup}(A(v_i))$ (gradient green brick with "drop" icon), v_i is added to $\tilde{A}_g$. **(c)** Otherwise, a vertex v_i with $|\bar{\texttt{A}}\texttt{2A}(v_i)| = 1$ is found. After similar removal, v_i is replaced by $\bar{\texttt{A}}\texttt{2A}(v_i)$, i.e., v_j and added to $\tilde{A}_g$.

Theorem 1. *For any two-colorable graph state $|G\rangle$, with corresponding graph $G = (P_1, P_2, E)$, Algorithm 1 determines:*

- *a lower bound $r^{\ell}_g(n)$ of the remote n-Gability volume and the location of the extracted n-qubit GHZ states,*
- *a lower bound r^{ℓ}_e of the remote Pairability volume and the location of the extracted EPR pairs,*

within a time complexity of $O(|P_1|^3 * |P_2|)$.

Proof: Please refer to App. B. ■

Corollary 4. *For any two-colorable graph state $|G\rangle$, with corresponding graph $G = (P_1, P_2, E)$, Algorithm 1 determines the maximum mass n_{max} of an extractable GHZ state among remote nodes with time complexity $O(|P_1| * |P_2|)$.*

Proof: Please refer to App. B. ■

Remark. Our algorithm leverages graph theory tools and uses only single-qubit Clifford operations, single-qubit Pauli measurement and classical communications. Theo. 1 shows that Alg. 1 can determine the volume and location of the vertices involved in the extracted entangled resources in polynomial-time. Furthermore, the maximum mass can also be obtained in polynomial time.
It is worthwhile to emphasize that Alg. 1 computes a lower bound on the volume of the extractable entangled resources. By summarizing, the volume of the remote n-Gability and remote Pairability of a general two-colorable graph state are

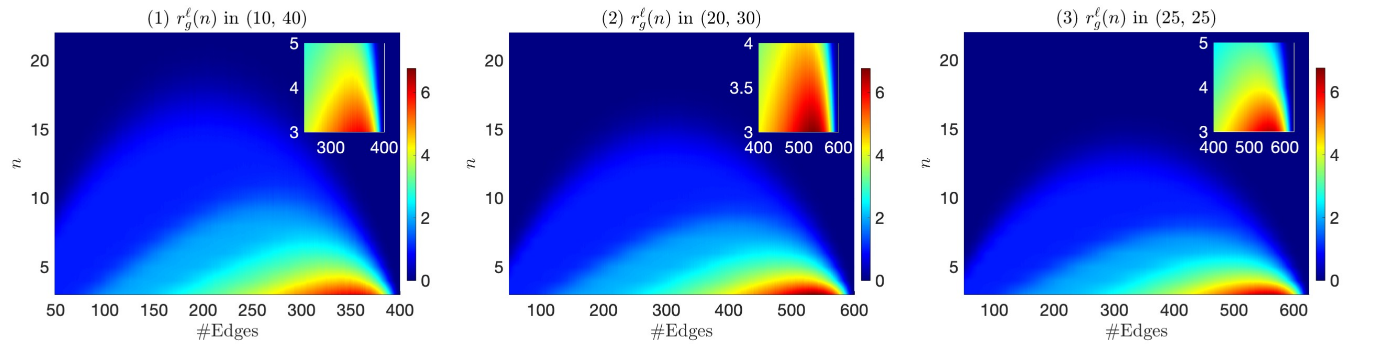

Fig. 6: Remote n-Gability Performance Analysis: Average volume $r_g^\ell(n)$ for different graph state partitions.

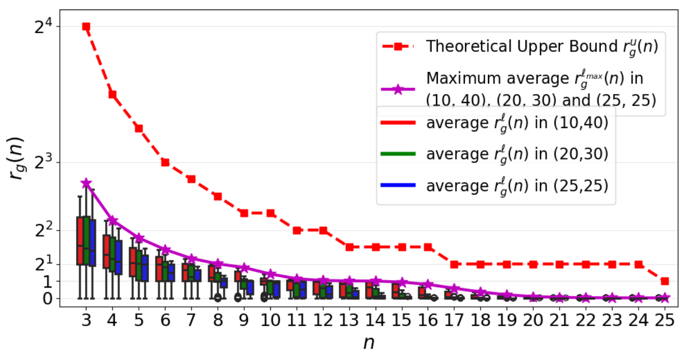

Fig. 7: Remote n-Gability Performance Analysis: The average constructive lower bound $r_g^\ell(n)$ of the volume against the theoretical upper bound $r_g^u(n)$.

constructively bounded as follows:

$$r_g^\ell(n) \text{ given in (22)} \leq r_g(n) \leq \lfloor \frac{N}{n} \rfloor, \tag{23}$$

$$r_e^\ell = r_g^\ell(2) \text{ given in (22)} \leq r_e \leq \lfloor \frac{N}{2} \rfloor. \tag{24}$$

This result is remarkable, since, as stated in Sec. I, no known algorithm – even with exponential-time complexity – guarantees an exact solution for all graph state structures. The underlying theoretical problem is indeed NP-complete.

V. Performance Evaluation

Here, we conduct a performance analysis, by considering general two-colorable graph states and representative Internet-inspired artificial topologies.

In light of the above remark, which highlights the absence of procedures to determine the exact solutions for the Remote VM-problem, our analysis is conducted in the worst-case scenario, by comparing our results against theoretical upper bounds. These upper bounds are inherently very conservative, being static and independent of the specific graph state instance. In contrast, the lower bounds computed by Algorithm 1 are not only constructive but are able to adapt to varying graph structures. To rigorously account for structural heterogeneity across graph instances, the results are averages over 1,000 independently generated graph instances.

A. General Two-colorable Graph State Performance

We first conducted a comprehensive evaluation of general two-colorable graph states under various graph structures. An explicit setup process is provided, along with a detailed analysis of remote pairability and remote n-Gability.

*1) **Setup**:* We evaluate the extractable values against different bipartite graph structures by randomly varying the number of edges m, while keeping the total number of nodes constant and equal to 50. This allows for a fair comparison across various graph instances. Furthermore, for the sake of generality, we distribute the nodes in different ways: one approach allocates nodes unequally across partitions, while the other ensures an equal number of nodes in each partition. More into details, we consider graphs with partitions (P_1, P_2) having sizes (10, 40), (20, 30), (25, 25), respectively. We then randomly distribute the m edges between the two partitions, thereby varying the graph structure. For being adherent to the definition of bipartite graph state, the number of edges in the corresponding graph has to satisfy following inequality:

$$(|P_1| + |P_2| - 1) \leq m \leq |P_1| * |P_2|, \tag{25}$$

and we generated 1000 random graphs per edge number scenario for statistical reliability.

*2) **Remote n-Gability Performance Analysis**:* To evaluate the volume for remote Gability, we compute via Algorithm 1 the average $r_g^\ell(n)$ in (22), which serves as constructive lower bound. Fig. 6 validates the n-Gability volume, for each configuration of bipartite graph state and against not only the number m of edges but also against the mass n of the extracted GHZ states. As shown in Fig. 6 the proposed approach generally allows for the extraction of at least one GHZ state with a mass ranging from 3 to 17 among remote nodes. This implies that for a given graph state, one can typically extract a GHZ state of significant size among distant parties. Notably, when we consider $|GHZ\rangle_3$, we observe that the $r_g^\ell(3)$ surpasses 6 for each considered partition-configuration of the graph state. This suggests that our approach facilitates the formation of small-scale GHZ states, i.e., of small subnets that can be exploited by entanglement-based protocols. Additionally, in Fig. 7, we present the theoretical upper bound and the maximum average extractable volume $r_g^\ell(n)$ for $n \in [3, 25]$ in graph states with partitions (10, 40), (20, 30), and (25, 25). As n increases,

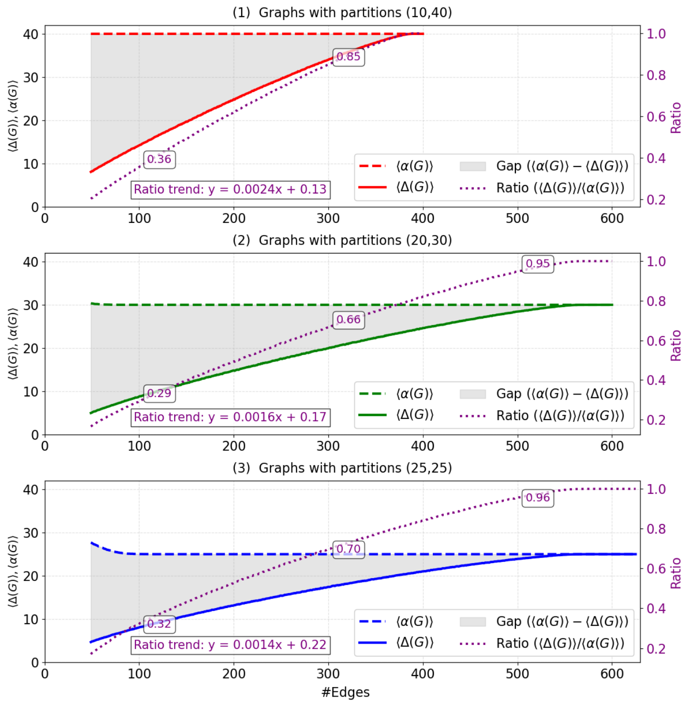

Fig. 8: Maximum Mass n_{max} of Remote n-Gability: Average lower- $\Delta(G)$ and upper $\alpha(G)$ bounds, for different graph partitions (10, 40), (20, 30), (25, 25), respectively.

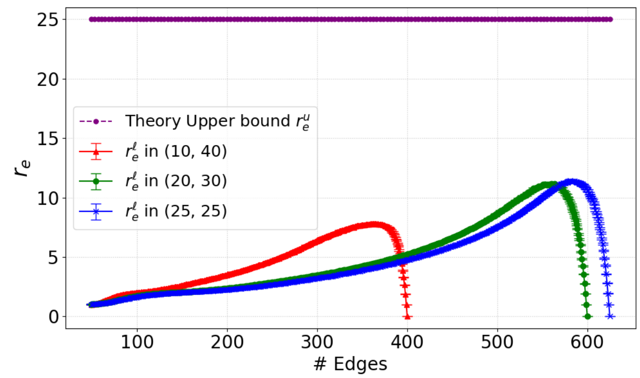

Fig. 9: Remote Pairability Performance Analysis I: 95% confidence interval of the volume lower-bound r_e^ℓ, with partitions (10, 40), (20, 30), (25, 25), respectively. The figure also shows the theoretical upper bound r_e^u, for the remote Pairability volume.

the gap between the two bounds diminishes, although the theoretical upper bound is inherently very conservative, being static and independent of the specific graph state instance. This confirms undirectly the tightness and efficacy of our constructive lower bounds.

Furthermore, we stress that existing studies focus on maximizing the mass of a single GHZ state, by limiting the volume to be equal to one. For a graph state $|G\rangle$ with bounded rank-width, in [50] a poly-time algorithm determines whether a GHZ state can be extracted using local Clifford operations and Z-measurements, providing the required operation sequence. Similarly, [19] demonstrates the extraction of GHZ states with masses from 4 to 11 starting from linear cluster states of up to 19 qubits on the IBMQ Montreal quantum device. By accounting for the above, our results not only demonstrate the extraction of GHZ states with significantly larger masses ranging from 3 to 17, but also ensure the extraction of a considerable volume of 3-qubit $|GHZ\rangle$ states. This showcases the versatility of our method, enabling both large and small-scale GHZ states, and providing a scalable and efficient approach for quantum networks.

Maximum Mass n_{max} Performance Analysis: To evaluate the extractable maximum mass for remote Gability, we compute the average lower bound $\Delta(G)$ and corresponding theoretical upper bound $\alpha(G)$, given in (20). Fig. 8 validates the mass analysis, for each configuration of bipartite graph state and against the edge number m. Specifically, both $\Delta(G)$ and $\alpha(G)$ are affected by the partition ratio ($|P_1| : |P_2|$). And as the partition ratio approaches 1, $\alpha(G)$ decreases. Notably, $\alpha(G)$ remains largely unaffected by the number of edges m, whereas for each bipartite graph configuration, $\Delta(G)$ increases with m and eventually converges to $\alpha(G)$. Intuitively, a more balanced partition ($|P_1| : |P_2|$ closer to 1) results in a smaller gap between $\Delta(G)$ and $\alpha(G)$. To illustrate this, we also plot the trend of the ratio in Fig. 8.

*3) **Remote Pairability Performance Analysis**:* To evaluate the remote Pairability for general two-colorable graph states, we compute the 95% confidence interval of the constructive lower-bound $r_g^\ell(2)$, given in (22). Specifically, in Fig. 9, we present both theoretical upper bound and our constructive lower bound. We observe an intriguing contrast in the performance of r_e^ℓ across the three different partitions size of graph states. Specifically, the (25, 25) configuration exhibits the highest r_e^ℓ values (11-12), indicating more pronounced extractable capabilities in balanced graph structures.

To demonstrate the effectiveness of our algorithm, in Fig. 10 we also compare the preliminary estimation $\tilde{r}_e = \tilde{r}_g(2)$ in (21) of the remote Pairability volume, provided in the Step 2.1 of Alg. 1, with the final constructive lower bound r_e^ℓ. The figure shows that r_e^ℓ is significantly higher that the initial estimation $\tilde{r}_e$, for all the three partition configurations. The aformentioned trend is observed by excluding, as expected, the sparse graph regime and the high density regime.

Related to the last observation, we further stress that the comparison between our bounds and existing literature is not fair, since our work is the first one, to the best of our knowledge, focusing on remote Pairability rather then on plain Pairability. More into details, regarding the Pariability, existing works, such as [35], [51], propose algorithms to determine whether subsets of Bell pairs can be extracted from graph states with specific structures, such as rings, lines, and trees. Indeed, [51] provides conditions for extracting two EPR pairs from these structures, but they do not ensure remote extraction. Similarly, [35] presents a 2-pairable 10-qubit graph state based on a "wheel graph" through exhaustive numerical evaluations of all the permutations of Pauli measurements on the qubits, without ensuring again remote extractions. Differently, with

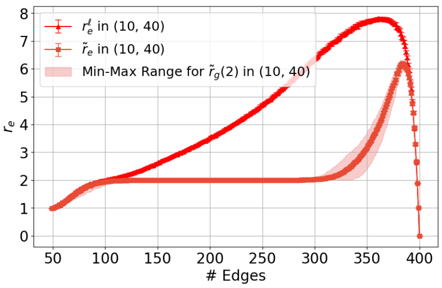

(a) Graphs with partitions $(10, 40)$.

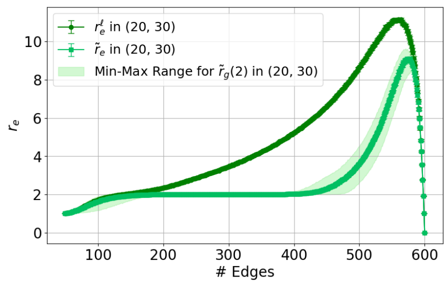

(b) Graphs with partitions $(20, 30)$.

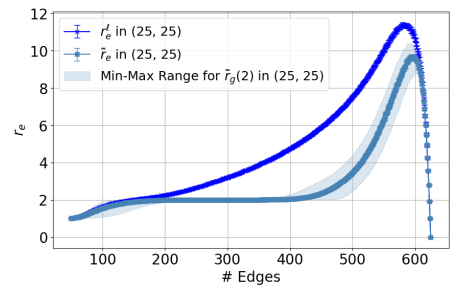

(c) Graphs with partitions $(25, 25)$.

Fig. 10: Remote Pairability Performance Analysis II: 95% confidence interval for r_e^ℓ against the preliminary estimation $\tilde{r}_e$ in (21), with volumes from Step 2.1 of Alg.1. The figure also shows min-max range of $\tilde{r}_e$ for each configuration of graph state.

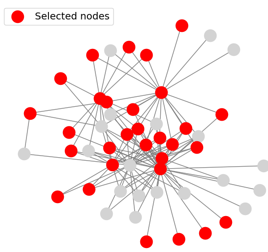

(a) Original PPI topology

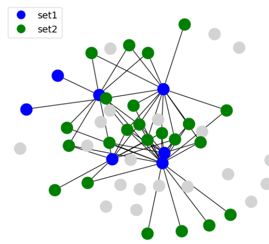

(b) Bipartite subgraph

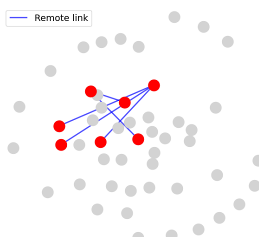

(c) Remote extracted entanglement resource

Fig. 11: Pictorial illustration for Remote extraction from general graph state. (a) The sample Protein-Protein Interactions (PPI) topology is generated by NetworkX library. (b) The extract bipartite subgraphs from PPI topology with fixed number of nodes. (c) The remote extracted entanglement resource, i.e., a 4-qubit GHZ and a 3-qubit GHZ, obtained by Alg. 1.

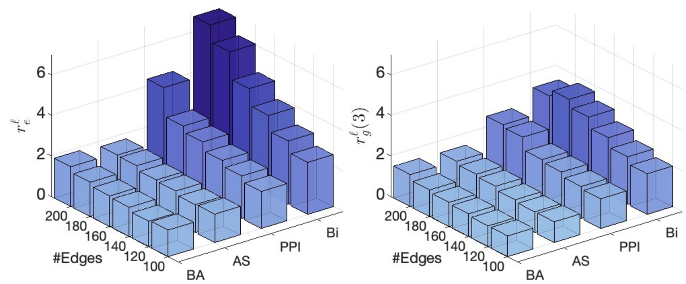

Fig. 12: Remote Pairability and Remote Gability Performance Analysis: Average extractable volume r_e^ℓ, $r_g^\ell(3)$ in general 50-qubit graph state with BA-model, AS Internet, Protein-Protein Interactions, and Bipartite network topology, respectively.

the same structure, our results assure one remote EPR extraction, through a significantly more constructive approach.

B. General Graph State Performance

In the following, we evaluate the extractable volume $r_e^\ell, r_g^\ell(n)$ in general graph state against different graph structures. To better reflect the tested graph structures expected in future quantum networks, we selected four representative Internet topologies, World Wide Web (with BA model), AS Internet, Protein-Protein Interactions, and Bipartite network topology, to serve as artificial topologies for tested graph states. For each of these topologies, we conduct evaluations on remote n-Gability and remote Pairability.

To ensure a fair and consistent evaluation across different topologies, we fix the total number of nodes at 50 and use the NetworkX library to generate graph instances by varying the number of edges m. However, as the original Internet topologies are not necessarily bipartite, Algorithm 1 cannot be directly applied to compute their extractable volumes. To address this, we extract bipartite subgraphs from each 50-node topology by selecting 30 nodes that form a bipartite graph as shown in Fig. 11. To ensure statistical reliability, we performed 100 experiments to generate random graphs for each edge number scenario. This allows for a fair comparison across topologies under consistent structural conditions.

To evaluate the remote Pairability for general graph states, we compute the average lower-bound r_e^ℓ, in Fig. 12. We observe that the volume can be successfully determined for each type of Internet topology. As the number of edges increases – i.e., as the network topology becomes denser – the extractable volume exhibits an approximately linear growth trend.

For remote n-Gability, we evaluate the extractable volume for 3-qubit GHZ states, i.e., $r_g^\ell(3)$, as a representative case. The results are shown in Fig. 12. Similar to the remote pairability case, we are able to determine the extractable volume for all tested Internet topologies. In general, the extractable volume increases roughly linearly with edge density. However, we also observe a performance drop in extremely dense bipartite network structures, where the extractable volume does not continue to increase and may slightly decline.

Appendix A
Proof of Lemma 1

We assume that equation (13) holds, and we must prove that $\dot{r}_g(n)$ GHZ states with each GHZ involving at least n qubits can be extracted from the graph state $|G\rangle$. Let us assume, without loss of generality, $A_g \subseteq V_1 \subseteq P_1$ and let us follow the labeling given in (8) and (9). Additionally, in the following, we denote with $N^i \triangleq N(v_1^i)$ and $\overline{N}^i \triangleq \overline{N}(v_1^i)$ the set of neighbors and the set of opposite remote nodes for node v_1^i in the original graph G, respectively. Conversely, we use $N(v_1^i)$ and $\overline{N}(v_1^i)$ for denoting the "current" identities of the nodes belonging to the respective sets during the manipulation of the graph. The proof constructively follows by performing the following four tasks. In a nutshell, the first two tasks remove irrelevant vertices which will not be linked by a GHZ state. The third task interconnects each vertex in A_g with its opposite remote set, with the exception of an arbitrary vertex. Finally, the last task interconnects also such a vertex with its opposite remote set and removes extra links among the nodes in A_g, as detailed in the following.

i) Pauli-z measurements on the qubits corresponding to the vertices in $V_1 \setminus A_g$ plus all the start vertices in S_1 except one vertex, say s_1^1.

ii) Pauli-z measurements on the qubits corresponding to the vertices in $V_2 \setminus \overline{N}_\cup(A_g)$ plus all the start vertices in S_2 except one vertex, say s_2^1.
These two tasks are equivalent to remove irrelevant vertices, which will not be linked by a GHZ state, with the exception of the two additional vertices, namely, s_1^1 and s_2^1. Thus, the former two tasks yield to the graph:

$$G' = G - \big(P_1 \setminus (A_g \cup \{s_1^1\})\big) - \big(P_2 \setminus (\overline{N}_\cup(A_g)) \setminus \{s_2^1\}\big). \tag{26}$$

iii) Pauli-X measurement on the selected star vertex s_2^1 with the arbitrary neighbor $k_0 \in A_g$, denoted as v_1^1 for the sake of simplicity. Thus, the third task yields the graph:

$$G'' = \tau_{v_1^1}\Big(\tau_{s_2^1}\big(\tau_{v_1^1}(G')\big) - s_2^1\Big). \tag{27}$$

iv) Pauli-X measurement on the star vertex s_1^1 by choosing again v_1^1 as the arbitrary neighbor k_0 (which belongs now to $N(s_1^1)$ as a consequence of the first Pauli-X measurement). Thus, the forth task yields the graph:

$$G''' = \tau_{v_1^1}\Big(\tau_{s_1^1}\big(\tau_{v_1^1}(G'')\big) - s_1^1\Big). \tag{28}$$

From (28), we have that, in the final graph, each node $v_1^i \in A_g$ is connected with and only with all the nodes in the original opposite remote set $\overline{N}^i$. Hence, by considering the subgraph induced by the vertices $\{v_1^i\} \cup \overline{N}^i$, such a subgraph is a star subgraph with v_1^i acting as star vertex, and each of these $\dot{r}_g(n) = |A_g|$ subgraphs is disconnected – i.e., disjoint – from the others subgraphs. Thus, the thesis follows.

Appendix B
Proof of Theorem 1

(1) Complexity for determining n_{max}^ℓ

The procedure (Lines 1-6) requires $O(|P_1| * |P_2|)$ time complexity to ensure each partition contains at least one star vertex. Then, the algorithm computes the lower bound of maximum mass n_{mass}, by evaluating the vertex degrees within the star sets S_1 and S_2, i.e., $n_{mass}^\ell = \max\{\deg(v) \mid v \in (S_1 \cup S_2)\}$. In fact, by definition, this is equal to $\Delta(G)$, namely the maximum degree of the graph. Accordingly, the procedure maintains an overall time complexity of $O(|P_1| * |P_2|)$.

(2) Complexity for determining $r_g^\ell(n)$ and the location of the involved vertices.

Lines 8-14: we firstly generate a random permutation of V_1, which exhibits a time-complexity of $O(|P_1|)$. Then the procedure constructs A_g, B_g, via sequential checks, which require a time complexity of $O(|P_1|^2 * |P_2|)$ in the worst case. Then, if the cardinality of B_g is larger than A_g, we remove the intersection of the opposite remote sets of B_g, namely $\overline{N}_\cap(B_g)$, from the vertex set. This exhibits a time complexity of $O(|P_1| * |P_2|)$, again in the worst case, i.e., for $|B_g| = |P_1|$.

Lines 15-34: The **`ExpandA`** subroutine, at line 15, firstly computes $\bar{A}$, which requires to calculate the opposite remote set for (in the worst case) each nodes in P_1. This in turn exhibits a time complexity of $O(|P_1| * |P_2|)$. Then, **`ExpandA`** constructs $\bar{\texttt{A}}\texttt{2A}$ and $\texttt{B2A}$ by per-element checks for each $v_i \in \bar{\texttt{A}}$. In total, this requires $O(|\bar{A}| * |\tilde{A}_g| * |P_2|)$ time, in the worst case, to compute $\bar{\texttt{A}}\texttt{2A}$. Similarly for $\texttt{B2A}$. The check condition, at Line 8 within the subroutine **`ExpandA`**, takes $O(|\texttt{B2A}(v_i)| * |P_2|)$. Overall, the construction of $\bar{\texttt{A}}\texttt{2A}$ and $\texttt{B2A}$ takes $O(|\bar{A}| * |P_1| * |P_2|) \subseteq O(|P_1|^2 * |P_2|)$.

After that, the procedures enters the `While` loop (Line 16-31 in Alg. 1), which exhibits two cases per iteration, namely, Case 1: $\texttt{A}(v_i) = \emptyset$ and Case 2: $\texttt{A}(v_i) \neq \emptyset$.

- Case 1 requires $O(\texttt{A})$ time for the vertex search.
- Case 2 computes the opposite remote set of a randomly selected vertex v_i in $O(|P_2|)$ time, and computes the union of opposite remote set of $\texttt{A}(v_i)$, i.e., in $O(|\tilde{A}_g| * |P_2|)$ (in the worst case). If $|\bar{\texttt{A}}\texttt{2A}(v_i)| = 1$, we need to spend $O(|P_2|)$ time to calculate the opposite remote set of v_j.

Then, both the cases recompute $\texttt{A}, \bar{\texttt{A}}\texttt{2A}$ via **`ExpandA`** in $O(|P_1|^2 * |P_2|)$ time. The `While` loop terminates when $\texttt{A}$ is empty, which in the worst-case, requires $O(|P_1|)$ iterations. Accordingly to the above, we can state that the total `While` loop complexity is $O(|P_1|^3 * |P_2|)$.

The procedure then takes $O(|\hat{A}_g| * |P_2|)$ time to map each vertex in $\hat{A}_g$ to its opposite remote-set in P_2. As a result, the location of each extracted resource can be identified as $\{v_i, \overline{N}(v_i)\}$, where $v_i \in \hat{A}_g$.

Based on above analysis, the dominant term is $O(|P_1|^3 * |P_2|)$. Thus, the time-complexity for determining the extractable volume $r_g^\ell(n)$ and the corresponding locations of the involved vertices in Alg. 1 is polynomial.

References

[1] S.-Y. Chen, A. S. Cacciapuoti, and M. Caleffi, "Polynomial-time extraction of entanglement resources," *under review for publication in conference proceedings*.

[2] A. S. Cacciapuoti, J. Illiano, and M. Caleffi, "Quantum internet addressing," *IEEE Network*, 2023.

[3] A. Pirker, J. Wallnöfer, and W. Dür, "Modular architectures for quantum networks," *New Journal of Physics*, vol. 20, no. 5, p. 053054, 2018.

[4] A. Pirker and W. Dür, "A quantum network stack and protocols for reliable entanglement-based networks," *New Journal of Physics*, vol. 21, no. 3, p. 033003, mar 2019.

[5] J. Illiano, M. Caleffi, A. Manzalini, and A. S. Cacciapuoti, "Quantum internet protocol stack: a comprehensive survey," *Computer Networks*, vol. 213, 2022.

[6] J. Miguel-Ramiro, A. Pirker, and W. Dür, "Genuine quantum networks with superposed tasks and addressing," *npj Quantum Information*, vol. 7, p. 135, 09 2021.

[7] C. Kruszynska, S. Anders, W. Dür, and H. J. Briegel, "Quantum communication cost of preparing multipartite entanglement," *Physical Review A*, vol. 73, no. 6, p. 062328, 2006.

[8] J. Illiano, M. Caleffi, M. Viscardi, and A. S. Cacciapuoti, "Quantum mac: Genuine entanglement access control via many-body dicke states," *IEEE Transactions on Communications*, vol. PP, pp. 1–1, 01 2023.

[9] M. Liu, Z. Li, K. Cai, J. Allcock, S. Zhang, and J. C. Lui, "Quantum bgp with online path selection via network benchmarking," in *IEEE INFOCOM 2024 - IEEE Conference on Computer Communications*, 2024, pp. 1401–1410.

[10] M. Liu, Z. Li, X. Wang, and J. C. S. Lui, "Linkselfie: Link selection and fidelity estimation in quantum networks," in *IEEE INFOCOM 2024 - IEEE Conference on Computer Communications*, 2024, pp. 1421–1430.

[11] F. Mazza, M. Caleffi, and A. S. Cacciapuoti, "Quantum LAN: On-Demand Network Topology via Two-colorable Graph States," *2024 QCNC*, pp. 127–134, 2024.

[12] S.-Y. Chen, J. Illiano, A. S. Cacciapuoti, and M. Caleffi, "Entanglement-based artificial topology: Neighboring remote network nodes," *IEEE OJ-COMS*, vol. 6, pp. 2220–2238, 2024.

[13] F. Mazza, M. Caleffi, and A. S. Cacciapuoti, "Intra-qlan connectivity via graph states: Beyond the physical topology," *IEEE Transactions on Network Science and Engineering*, 2025.

[14] S.-Y. Chen, J. Illiano, A. S. Cacciapuoti, and M. Caleffi, "Scaling quantum networks: Inter-qlans artificial connectivity," in *2024 IEEE International Conference on Quantum Computing and Engineering*, vol. 1, 2024, pp. 1980–1988.

[15] A. S. Cacciapuoti, M. Caleffi, R. Van Meter, and L. Hanzo, "When entanglement meets classical communications: Quantum teleportation for the quantum internet," *IEEE Transactions on Communications*, vol. 68, no. 6, pp. 3808–3833, 2020, invited paper.

[16] V. Mannalath and A. Pathak, "Multiparty entanglement routing in quantum networks," *Phys. Rev. A*, vol. 108, p. 062614, Dec 2023.

[17] H. J. Briegel and R. Raussendorf, "Persistent entanglement in arrays of interacting particles," *Phys. Rev. Lett.*, vol. 86, pp. 910–913, Jan 2001.

[18] R. Frantzeskakis, C. Liu, Z. Raissi, E. Barnes, and S. E. Economou, "Extracting perfect ghz states from imperfect weighted graph states via entanglement concentration," *Phys. Rev. Res.*, vol. 5, p. 023124, 2023.

[19] J. de Jong, F. Hahn, N. Tcholtchev, M. Hauswirth, and A. Pappa, "Extracting ghz states from linear cluster states," *Physical Review Research*, vol. 6, no. 1, p. 013330, 2024.

[20] E. A. Van Milligen, C. N. Gagatsos, E. Kaur, D. Towsley, and S. Guha, "Utilizing probabilistic entanglement between sensors in quantum networks," *Physical Review Applied*, vol. 22, no. 6, Dec. 2024.

[21] M. Christandl and S. Wehner, "Quantum anonymous transmissions," in *Advances in Cryptology - ASIACRYPT 2005*, B. Roy, Ed. Berlin, Heidelberg: Springer Berlin Heidelberg, 2005, pp. 217–235.

[22] D. Markham and B. C. Sanders, "Graph states for quantum secret sharing," *Phys. Rev. A*, vol. 78, p. 042309, 2008.

[23] G. Murta, F. Grasselli, H. Kampermann, and D. Bruß, "Quantum conference key agreement: A review," *Advanced Quantum Technologies*, vol. 3, no. 11, p. 2000025, 2020.

[24] F. Hahn, J. de Jong, and A. Pappa, "Anonymous quantum conference key agreement," *PRX Quantum*, vol. 1, p. 020325, Dec 2020.

[25] M. Pompili, S. L. Hermans, S. Baier, H. K. Beukers, P. C. Humphreys, R. N. Schouten, R. F. Vermeulen, M. J. Tiggelman, L. dos Santos Martins, B. Dirkse *et al.*, "Realization of a multinode quantum network of remote solid-state qubits," *Science*, vol. 372, no. 6539, 2021.

[26] S. Hermans, M. Pompili, H. Beukers, S. Baier, J. Borregaard, and R. Hanson, "Qubit teleportation between non-neighbouring nodes in a quantum network," *Nature*, vol. 605, no. 7911, pp. 663–668, 2022.

[27] C. Li, T. Li, Y.-X. Liu, and P. Cappellaro, "Effective routing design for remote entanglement generation on quantum networks," *npj Quantum Information*, vol. 7, no. 1, p. 10, 2021.

[28] P. C. Humphreys, N. Kalb, J. P. Morits, R. N. Schouten, R. F. Vermeulen, D. J. Twitchen, M. Markham, and R. Hanson, "Deterministic delivery of remote entanglement on a quantum network," *Nature*, vol. 558, no. 7709, pp. 268–273, 2018.

[29] N. Benchasattabuse, M. Hajdušek, and R. Van Meter, "Architecture and protocols for all-photonic quantum repeaters," in *2024 IEEE International Conference on Quantum Computing and Engineering (QCE)*, vol. 1. IEEE, 2024, pp. 1879–1889.

[30] M. Hein, W. Dür, J. Eisert, R. Raussendorf, M. Van den Nest, and H.-J. Briegel, "Entanglement in graph states and its applications," in *Quantum computers, algorithms and chaos*. IOS Press, 2006, pp. 115–218.

[31] H.-J. Briegel, "Multiparticle entanglement purification for two-colorable graph states," *Physical Review A*, vol. 71, no. 1, p. 012319, 2005.

[32] Z. Tang, P. Zhang, W. O. Krawec, and L. Wang, "Quantum networks for resilient power grids: Theory and simulated evaluation," *IEEE Transactions on Power Systems*, vol. 38, no. 2, pp. 1189–1204, 2023.

[33] J. Freund, A. Pirker, and W. Dür, "A flexible quantum data bus," *arXiv preprint arXiv:2404.06578*, 2024.

[34] F. Hahn, A. Pappa, and J. Eisert, "Quantum network routing and local complementation," *npj Quantum Information*, vol. 5, no. 1, p. 76, 2019.

[35] S. Bravyi, Y. Sharma, M. Szegedy, and R. de Wolf, "Generating k epr-pairs from an n-party resource state," *arXiv:2211.06497*, 2022.

[36] K. Azuma, K. Tamaki, and H.-K. Lo, "All-photonic quantum repeaters," *Nature communications*, vol. 6, no. 1, pp. 1–7, 2015.

[37] F. Mazza, C. Zhan, J. Chung, R. Kettimuthu, M. Caleffi, and A. S. Cacciapuoti, "Simulation of entanglement-enabled connectivity in qlans using sequence," in *ICC 2025 - IEEE International Conference on Communications*, 2025.

[38] A. Dahlberg, J. Helsen, and S. Wehner, "Transforming graph states to bell-pairs is np-complete," *Quantum*, vol. 4, p. 348, 2020.

[39] M. Cautrès, N. Claudet, M. Mhalla, S. Perdrix, V. Savin, and S. Thomassé, "Vertex-minor universal graphs for generating entangled quantum subsystems," *arXiv preprint arXiv:2402.06260*, 2024.

[40] A. Dahlberg, J. Helsen, and S. Wehner, "How to transform graph states using single-qubit operations: computational complexity and algorithms," *Quantum Science and Technology*, vol. 5, no. 4, 2020.

[41] M. Dyer and C. Greenhill, "On markov chains for independent sets," *Journal of Algorithms*, vol. 35, no. 1, pp. 17–49, 2000.

[42] M. Xia, P. Zhang, and W. Zhao, "Computational complexity of counting problems on 3-regular planar graphs," *Theoretical Computer Science*, vol. 384, no. 1, pp. 111–125, 2007.

[43] S. Cannon and W. Perkins, "Counting independent sets in unbalanced bipartite graphs," *ArXiv*, vol. abs/1906.01666, 2019.

[44] M. Hein, J. Eisert, and H. J. Briegel, "Multiparty entanglement in graph states," *Physical Review A*, vol. 69, no. 6, p. 062311, 2004.

[45] M. Van den Nest, W. Dür, and H. J. Briegel, "Completeness of the classical 2d ising model and universal quantum computation," *Physical review letters*, vol. 100, no. 11, p. 110501, 2008.

[46] M. Van den Nest, J. Dehaene, and B. De Moor, "Graphical description of the action of local clifford transformations on graph states," *Phys. Rev. A*, vol. 69, p. 022316, Feb 2004.

[47] K. Chen and H.-K. Lo, "Multi-partite quantum cryptographic protocols with noisy ghz states," *Quantum Info. Comput.*, vol. 7, no. 8, 2007.

[48] A. R. Calderbank and P. W. Shor, "Good quantum error-correcting codes exist," *Physical Review A*, vol. 54, no. 2, p. 1098, 1996.

[49] A. M. Steane, "Error correcting codes in quantum theory," *Physical Review Letters*, vol. 77, no. 5, p. 793, 1996.

[50] S.-I. Oum, "Approximating rank-width and clique-width quickly," *ACM Trans. Algorithms*, vol. 5, no. 1, Dec. 2008.

[51] D. Zhang, "Bell pair extraction using graph foliage techniques," *Journal of Mathematical Physics*, vol. 66, no. 2, 2025.